

¹ **Power laws and critical transitions in global forests**

² **Leonardo A. Saravia^{1 3}, Santiago R. Doyle¹, Ben Bond-Lamberty²**

³ 1. Instituto de Ciencias, Universidad Nacional de General Sarmiento, J.M. Gutierrez 1159 (1613), Los
⁴ Polvorines, Buenos Aires, Argentina.

⁵ 2. Pacific Northwest National Laboratory, Joint Global Change Research Institute at the University of
⁶ Maryland–College Park, 5825 University Research Court #3500, College Park, MD 20740, USA

⁷ 3. Corresponding author e-mail: lsaravia@ungs.edu.ar

⁸ **Keywords:** Forest fragmentation, early warning signals, percolation, power-laws, MODIS, critical transitions

⁹ **Running title:** Critical fragmentation in global forest

¹⁰ **Abstract**

¹¹ 1. Forests provide critical habitat for many species, essential ecosystem services, and are coupled to
¹² atmospheric dynamics through exchanges of energy, water and gases. One of the most important
¹³ changes produced in the biosphere is the replacement of forest areas with human dominated landscapes.
¹⁴ This usually leads to fragmentation, altering the sizes of patches, the structure and function of the
¹⁵ forest. Here we studied the distribution and dynamics of forest patch sizes at a global level, examining
¹⁶ signals of a critical transition from an unfragmented to a fragmented state.

¹⁷ 2. We used MODIS vegetation continuous field to estimate the forest patches at a global level and de-
¹⁸ fined wide regions of connected forest across continents and big islands. We search for critical phase
¹⁹ transitions, where the system state of the forest changes suddenly at a critical point in time; this
²⁰ implies an abrupt change in connectivity that causes an increased fragmentation level. We combined
²¹ five criteria to evaluate the closeness of the system to a fragmentation threshold, studying in particular
²² the distribution of forest patch sizes and the dynamics of the largest patch over the last sixteen years.

²³ 3. We found some necessary evidence that allows us to analyze fragmentation as a critical transition: all
²⁴ regions followed a power-law distribution over the fifteen years. We also found that the Philippines
²⁵ region probably went through a critical transition from a fragmented to an unfragmented state. Regions
²⁶ with the highest deforestation rates—South America, Southeast Asia, Africa—all met the criteria to
²⁷ be near a critical fragmentation threshold.

²⁸ 4. This implies that human pressures and climate forcings might trigger undesired effects of fragmentation,
²⁹ such as species loss and degradation of ecosystems services, in these regions. The simple criteria
³⁰ proposed here could be used as an early warning to estimate the distance to a fragmentation threshold
³¹ in forests around the globe.

³² Introduction

³³ Forests are one of the most important biomes on earth, providing habitat for a large proportion of species
³⁴ and contributing extensively to global biodiversity (Crowther *et al.* 2015). In the previous century human
³⁵ activities have influenced global bio-geochemical cycles (Bonan 2008; Canfield *et al.* 2010), with one of
³⁶ the most dramatic changes being the replacement of 40% of Earth's formerly biodiverse land areas with
³⁷ landscapes that contain only a few species of crop plants, domestic animals and humans (Foley *et al.* 2011).
³⁸ These local changes have accumulated over time and now constitute a global forcing (Barnosky *et al.* 2012).
³⁹ Another global scale forcing that is tied to habitat destruction is fragmentation, which is defined as the
⁴⁰ division of a continuous habitat into separated portions that are smaller and more isolated. Fragmentation
⁴¹ produces multiple interwoven effects: reductions of biodiversity between 13% and 75%, decreasing forest
⁴² biomass, and changes in nutrient cycling (Haddad *et al.* 2015). The effects of fragmentation are not only
⁴³ important from an ecological point of view but also that of human activities, as ecosystem services are deeply
⁴⁴ influenced by the level of landscape fragmentation (Rudel *et al.* 2005; Angelsen 2010; Mitchell *et al.* 2015).

⁴⁵ Ecosystems have complex interactions between species and present feedbacks at different levels of organization
⁴⁶ (Gilman *et al.* 2010), and external forcings can produce abrupt changes from one state to another, called
⁴⁷ critical transitions (Scheffer *et al.* 2009). These abrupt state shifts cannot be linearly forecasted from past
⁴⁸ changes, and are thus difficult to predict and manage (Scheffer *et al.* 2009). Such 'critical' transitions have
⁴⁹ been detected mostly at local scales (Drake & Griffen 2010; Carpenter *et al.* 2011), but the accumulation of
⁵⁰ changes in local communities that overlap geographically can propagate and theoretically cause an abrupt
⁵¹ change of the entire system at larger scales (Barnosky *et al.* 2012). Coupled with the existence of global
⁵² scale forcings, this implies the possibility that a critical transition could occur at a global scale (Rockstrom
⁵³ *et al.* 2009; Folke *et al.* 2011).

⁵⁴ Complex systems can experience two general classes of critical transitions (Solé 2011). In so-called first
⁵⁵ order transitions, a catastrophic regime shift that is mostly irreversible occurs because of the existence of
⁵⁶ alternative stable states (Scheffer *et al.* 2001). This class of transitions is suspected to be present in a variety
⁵⁷ of ecosystems such as lakes, woodlands, coral reefs (Scheffer *et al.* 2001), semi-arid grasslands (Bestelmeyer
⁵⁸ *et al.* 2011), and fish populations (Vasilakopoulos & Marshall 2015). They can be the result of positive
⁵⁹ feedback mechanisms (Villa Martín *et al.* 2015); for example, fires in some forest ecosystems were more
⁶⁰ likely to occur in previously burned areas than in unburned places (Kitzberger *et al.* 2012).

⁶¹ The other class of critical transitions are continuous or second order transitions (Solé & Bascompte 2006). In
⁶² these cases, there is a narrow region where the system suddenly changes from one domain to another, with

the change being continuous and in theory reversible. This kind of transitions were suggested to be present in tropical forests (Pueyo *et al.* 2010), semi-arid mountain ecosystems (McKenzie & Kennedy 2012), and tundra shrublands (Naito & Cairns 2015). The transition happens at a critical point where we can observe a distinctive spatial pattern: scale invariant fractal structures characterized by power law patch distributions (Stauffer & Aharony 1994). There are several processes that can convert a catastrophic transition to a second order transitions (Villa Martín *et al.* 2015). These include stochasticity, such as demographic fluctuations, spatial heterogeneities, and/or dispersal limitation. All these components are present in forest around the globe (Seidler & Plotkin 2006; Filotas *et al.* 2014; Fung *et al.* 2016), and thus continuous transitions might be more probable than catastrophic transitions. Moreover there is some evidence of recovery in some systems that supposedly suffered an irreversible transition produced by overgrazing (Zhang *et al.* 2005; Bestelmeyer *et al.* 2013) and desertification (Allington & Valone 2010).

The spatial phenomena observed in continuous critical transitions deal with connectivity, a fundamental property of general systems and ecosystems from forests (Ochoa-Quintero *et al.* 2015) to marine ecosystems (Leibold & Norberg 2004) and the whole biosphere (Lenton & Williams 2013). When a system goes from a fragmented to a connected state we say that it percolates (Solé 2011). Percolation implies that there is a path of connections that involves the whole system. Thus we can characterize two domains or phases: one dominated by short-range interactions where information cannot spread, and another in which long range interactions are possible and information can spread over the whole area. (The term “information” is used in a broad sense and can represent species dispersal or movement.) Thus, there is a critical “percolation threshold” between the two phases, and the system could be driven close to or beyond this point by an external force; climate change and deforestation are the main forces that could be the drivers of such a phase change in contemporary forests (Bonan 2008; Haddad *et al.* 2015). There are several applications of this concept in ecology: species’ dispersal strategies are influenced by percolation thresholds in three-dimensional forest structure (Solé *et al.* 2005), and it has been shown that species distributions also have percolation thresholds (He & Hubbell 2003). This implies that pushing the system below the percolation threshold could produce a biodiversity collapse (Bascompte & Solé 1996; Solé *et al.* 2004; Pardini *et al.* 2010); conversely, being in a connected state (above the threshold) could accelerate the invasion of forest into prairie (Loehle *et al.* 1996; Naito & Cairns 2015).

One of the main challenges with systems that can experience critical transitions—of any kind—is that the value of the critical threshold is not known in advance. In addition, because near the critical point a small change can precipitate a state shift of the system, they are difficult to predict. Several methods have been developed to detect if a system is close to the critical point, e.g. a deceleration in recovery from perturbations,

95 or an increase in variance in the spatial or temporal pattern (Hastings & Wysham 2010; Carpenter *et al.*
96 2011; Boettiger & Hastings 2012; Dai *et al.* 2012).

97 The existence of a critical transition between two states has been established for forest at a global scale in
98 different works (Hirotा *et al.* (2011); Staal *et al.* (2016); Wuyts *et al.* (2017)). It is generally believed that
99 this constitutes a first order catastrophic transition. The regions where forest can grow are not distributed
100 homogeneously, as there are demographic fluctuations in forest growth and disturbances produced by human
101 activities. Due to new theoretical advances (Villa Martín *et al.* 2014, 2015) all these factors imply that if
102 these were first order transitions they will be converted or observed as second order continuous transitions.
103 Recently, percolation theory has been suggested as an explanation of power law forest fragments (Taubert
104 *et al.* 2018). From this basis, we applied indices derived from second order transitions to global forest cover
105 dynamics.

106 In this study, our objective is to look for evidence that forests around the globe are near continuous critical
107 points that represent a fragmentation threshold. We use the framework of percolation to first evaluate if
108 forest patch distribution at a continental scale is described by a power law distribution and then examine
109 the fluctuations of the largest patch. The advantage of using data at a continental scale is that for very large
110 systems the transitions are very sharp (Solé 2011) and thus much easier to detect than at smaller scales,
111 where noise can mask the signals of the transition.

112 Methods

113 Study areas definition

114 We analyzed mainland forests at a continental scale, covering the whole globe, by delimiting land areas with
115 a near-contiguous forest cover, separated with each other by large non-forested areas. Using this criterion,
116 we delimited the following forest regions. In America, three regions were defined: South America temperate
117 forest (SAT), subtropical and tropical forest up to Mexico (SAST), and USA and Canada forest (NA). Europe
118 and North Asia were treated as one region (EUAS). The rest of the delimited regions were South-east Asia
119 (SEAS), Africa (AF), and Australia (OC). We also included in the analysis islands larger than 10^5km^2 . The
120 mainland region has the number 1 e.g. OC1, and the nearby islands have consecutive numeration (Appendix
121 S4, figure S1-S6). We applied this criterion to delimit regions because we based our study on percolation
122 theory that assumes some kind of connectivity in the study area (see below).

123 **Forest patch distribution**

124 We studied forest patch distribution in each defined area from 2000 to 2015 using the MODerate-resolution
125 Imaging Spectroradiometer (MODIS) Vegetation Continuous Fields (VCF) Tree Cover dataset version 051
126 (DiMiceli *et al.* 2015). This dataset is produced at a global level with a 231-m resolution, from 2000 onwards
127 on an annual basis, the last available year was 2015. There are several definition of forest based on percent
128 tree cover (Sexton *et al.* 2015); we choose a range from 20% to 40% threshold in 5% increments to convert
129 the percentage tree cover to a binary image of forest and non-forest pixels. This range is centered in the
130 definition used by the United Nations' International Geosphere-Biosphere Programme (Belward 1996), and
131 studies of global fragmentation (Haddad *et al.* 2015) and includes the range used in other studies of critical
132 transitions (Xu *et al.* 2016). Using this range we try to avoid the errors produced by low discrimination
133 of MODIS VCF between forest and dense herbaceous vegetation at low forest cover and the saturation of
134 MODIS VCF in dense forests (Sexton *et al.* 2013). We repeat all the analysis for this set of thresholds,
135 except in some specific cases described below. Patches of contiguous forest were determined in the binary
136 image by grouping connected forest pixels using a neighborhood of 8 forest units (Moore neighborhood).
137 The MODIS VCF product defines the percentage of tree cover by pixel, but does not discriminate the type
138 of trees so besides natural forest it includes plantations of tree crops like rubber, oil palm, eucalyptus and
139 other managed stands (Hansen *et al.* 2014).

140 **Percolation theory**

141 A more in-depth introduction to percolation theory can be found elsewhere (Stauffer & Aharony 1994) and a
142 review from an ecological point of view is available (Oborny *et al.* 2007). Here, to explain the basic elements
143 of percolation theory we formulate a simple model: we represent our area of interest by a square lattice
144 and each site of the lattice can be occupied—e.g. by forest—with a probability p . The lattice will be more
145 occupied when p is greater, but the sites are randomly distributed. We are interested in the connection
146 between sites, so we define a neighborhood as the eight adjacent sites surrounding any particular site. The
147 sites that are neighbors of other occupied sites define a patch. When there is a patch that connects the
148 lattice from opposite sides, it is said that the system percolates. When p is increased from low values, a
149 percolating patch suddenly appears at some value of p called the critical point p_c .

150 Thus percolation is characterized by two well defined phases: the unconnected phase when $p < p_c$ (called
151 subcritical in physics), in which species cannot travel far inside the forest, as it is fragmented; in a general
152 sense, information cannot spread. The second is the connected phase when $p > p_c$ (supercritical), species

153 can move inside a forest patch from side to side of the area (lattice), i.e. information can spread over the
154 whole area. Near the critical point several scaling laws arise: the structure of the patch that spans the area
155 is fractal, the size distribution of the patches is power-law, and other quantities also follow power-law scaling
156 (Stauffer & Aharony 1994).

157 The value of the critical point p_c depends on the geometry of the lattice and on the definition of the
158 neighborhood, but other power-law exponents only depend on the lattice dimension. Close to the critical
159 point, the distribution of patch sizes is:

160 (1) $n_s(p_c) \propto s^{-\alpha}$

161 where $n_s(p)$ is the number of patches of size s . The exponent α does not depend on the details of the
162 model and it is called universal (Stauffer & Aharony 1994). These scaling laws can be applied for landscape
163 structures that are approximately random, or at least only correlated over short distances (Gastner *et al.*
164 2009). In physics this is called “isotropic percolation universality class”, and corresponds to an exponent
165 $\alpha = 2.05495$. If we observe that the patch size distribution has another exponent it will not belong to this
166 universality class and some other mechanism should be invoked to explain it. Percolation thresholds can also
167 be generated by models that have some kind of memory (Hinrichsen 2000; Ódor 2004): for example, a patch
168 that has been exploited for many years will recover differently than a recently deforested forest patch. In
169 this case, the system could belong to a different universality class, or in some cases there is no universality,
170 in which case the value of α will depend on the parameters and details of the model (Corrado *et al.* 2014).

171 To illustrate these concepts, we conducted simulations with a simple forest model with only two states: forest
172 and non-forest. This type of model is called a “contact process” and was introduced for epidemics (Harris
173 1974), but has many applications in ecology (Solé & Bascompte 2006; Gastner *et al.* 2009). A site with forest
174 can become extinct with probability e , and produce another forest site in a neighborhood with probability
175 c . We use a neighborhood defined by an isotropic power law probability distribution. We defined a single
176 control parameter as $\lambda = c/e$ and ran simulations for the subcritical fragmentation state $\lambda < \lambda_c$, with $\lambda = 2$,
177 near the critical point for $\lambda = 2.5$, and for the supercritical state with $\lambda = 5$ (see supplementary data, gif
178 animations).

179 **Patch size distributions**

180 We fitted the empirical distribution of forest patches calculated for each of the thresholds on the range we
181 previously mentioned. We used maximum likelihood (Goldstein *et al.* 2004; Clauset *et al.* 2009) to fit four
182 distributions: power-law, power-law with exponential cut-off, log-normal, and exponential. We assumed

183 that the patch size distribution is a continuous variable that was discretized by the remote sensing data
184 acquisition procedure.

185 We set a minimal patch size (X_{min}) at nine pixels to fit the patch size distributions to avoid artifacts at patch
186 edges due to discretization (Weerman *et al.* 2012). Besides this hard X_{min} limit we set due to discretization,
187 the power-law distribution needs a lower bound for its scaling behavior. This lower bound is also estimated
188 from the data by maximizing the Kolmogorov-Smirnov (KS) statistic, computed by comparing the empirical
189 and fitted cumulative distribution functions (Clauset *et al.* 2009). For the log-normal model we constrain
190 the values of the μ parameter to positive values, this parameter controls the mode of the distribution and
191 when is negative most of the probability density of the distribution lies outside the range of the forest patch
192 size data (Limpert *et al.* 2001).

193 To select the best model we calculated corrected Akaike Information Criteria (AIC_c) and Akaike weights
194 for each model (Burnham & Anderson 2002). Akaike weights (w_i) are the weight of evidence in favor of
195 model i being the actual best model given that one of the N models must be the best model for that set of
196 N models. Additionally, we computed a likelihood ratio test (Vuong 1989; Clauset *et al.* 2009) of the power
197 law model against the other distributions. We calculated bootstrapped 95% confidence intervals (Crawley
198 2012) for the parameters of the best model, using the bias-corrected and accelerated (BCa) bootstrap (Efron
199 & Tibshirani 1994) with 10000 replications.

200 Largest patch dynamics

201 The largest patch is the one that connects the highest number of sites in the area. This has been used
202 extensively to indicate fragmentation (Gardner & Urban 2007; Ochoa-Quintero *et al.* 2015). The relation
203 of the size of the largest patch S_{max} to critical transitions has been extensively studied in relation to
204 percolation phenomena (Stauffer & Aharony 1994; Bazant 2000; Botet & Ploszajczak 2004), but is seldom
205 used in ecological studies (for an exception see Gastner *et al.* (2009)). When the system is in a connected
206 state ($p > p_c$) the landscape is almost insensitive to the loss of a small fraction of forest, but close to the
207 critical point a minor loss can have important effects (Solé & Bascompte 2006; Oborny *et al.* 2007), because
208 at this point the largest patch will have a filamentary structure, i.e. extended forest areas will be connected
209 by thin threads. Small losses can thus produce large fluctuations.

210 One way to evaluate the fragmentation of the forest is to calculate the proportion of the largest patch against
211 the total area (Keitt *et al.* 1997). The total area of the regions we are considering (Appendix S4, figures
212 S1-S6) may not be the same as the total area that the forest could potentially occupy, and thus a more

213 accurate way to evaluate the weight of S_{max} is to use the total forest area, which can be easily calculated
214 by summing all the forest pixels. We calculate the proportion of the largest patch for each year, dividing
215 S_{max} by the total forest area of the same year: $RS_{max} = S_{max} / \sum_i S_i$. This has the effect of reducing the
216 S_{max} fluctuations produced due to environmental or climatic changes influences in total forest area. When
217 the proportion RS_{max} is large (more than 60%) the largest patch contains most of the forest so there are
218 fewer small forest patches and the system is probably in a connected phase. Conversely, when it is low (less
219 than 20%), the system is probably in a fragmented phase (Saravia & Momo 2017). To define if a region will
220 be in a connected or unconnected state we used the RS_{max} of the highest (i.e., most conservative) threshold
221 of 40%, that represent the most dense area of forest within our chosen range. We assume that there are
222 two alternative states for the critical transition—the forest could be fragmented or unfragmented. If RS_{max}
223 is a good indicator of the fragmentation state of the forest its distribution of frequencies should be bimodal
224 (Bestelmeyer *et al.* 2011), so we apply the Hartigan's dip test that measures departures from unimodality
225 (Hartigan & Hartigan 1985).

226 The RS_{max} is a useful qualitative index that does not tell us if the system is near or far from the critical
227 transition; this can be evaluated using the temporal fluctuations. We calculate the fluctuations around the
228 mean with the absolute values $\Delta S_{max} = S_{max}(t) - \langle S_{max} \rangle$, using the proportions of RS_{max} . To characterize
229 fluctuations we fitted three empirical distributions: power-law, log-normal, and exponential, using the same
230 methods described previously. We expect that large fluctuation near a critical point have heavy tails (log-
231 normal or power-law) and that fluctuations far from a critical point have exponential tails, corresponding to
232 Gaussian processes (Rooij *et al.* 2013). As the data set spans 16 years, it is probable that we will not have
233 enough power to reliably detect which distribution is better (Clauset *et al.* 2009). To improve this we used
234 the same likelihood ratio test we used previously (Vuong 1989; Clauset *et al.* 2009); if the p-values obtained
235 to compare the best distribution against the others are not significant we concluded that there is not enough
236 data to decide which is the best model. We generated animated maps showing the fluctuations of the two
237 largest patches at 30% threshold, to aid in the interpretations of the results.

238 A robust way to detect if the system is near a critical transition is to analyze the increase in variance of the
239 density (Benedetti-Cecchi *et al.* 2015)—in our case ‘density’ is the total forest cover divided by the area. It
240 has been demonstrated that the variance increase in the density of patches appears when the system is very
241 close to the transition (Corrado *et al.* 2014), and thus practically it does not constitute an early warning
242 indicator. An alternative is to analyze the variance of the fluctuations of the largest patch ΔS_{max} : the
243 maximum is attained at the critical point but a significant increase occurs well before the system reaches the
244 critical point (Corrado *et al.* 2014; Saravia & Momo 2017). In addition, before the critical fragmentation,

245 the skewness of the distribution of ΔS_{max} should be negative, implying that fluctuations below the average
246 are more frequent. We characterized the increase in the variance using quantile regression: if variance is
247 increasing the slopes of upper or/and lower quartiles should be positive or negative.

248 All statistical analyses were performed using the GNU R version 3.3.0 (R Core Team 2015), to fit the
249 distributions of patch sizes we used the Python package powerlaw (Alstott *et al.* 2014). For the quantile
250 regressions we used the R package quantreg (Koenker 2016). Image processing was done in MATLAB r2015b
251 (The Mathworks Inc.). The complete source code for image processing and statistical analysis, and the patch
252 size data files are available at figshare <http://dx.doi.org/10.6084/m9.figshare.4263905>.

253 Results

254 The figure 1 shows an example of the distribution of the biggest 200 patches for years 2000 and 2014. This
255 distribution is highly variable; the biggest patch usually maintains its spatial location, but sometimes it
256 breaks and then big temporal fluctuations in its size are observed, as we will analyze below. Smaller patches
257 can merge or break more easily so they enter or leave the list of 200, and this is why there is a color change
258 across years.

259 The power law distribution was selected as the best model in 99% of the cases (Figure S7). In a small
260 number of cases (1%) the power law with exponential cutoff was selected, but the value of the parameter α
261 was similar by ± 0.03 to the pure power law (Table S1, and model fit data table). Additionally the patch size
262 where the exponential tail begins is very large, and thus we used the power law parameters for these cases
263 (region EUAS3,SAST2). In finite-size systems the favored model should be the power law with exponential
264 cut-off, because the power-law tails are truncated to the size of the system (Stauffer & Aharony 1994). This
265 implies that differences between the two kinds of power law models should be small. We observe this effect:
266 when the pure power-law model is selected as the best model the likelihood ratio test shows that in 64% of
267 the cases the differences with power law with exponential cutoff are not significant ($p\text{-value}>0.05$); in these
268 cases the differences between the fitted α for both models are less than 0.001. Instead the likelihood ratio
269 test clearly differentiates the power law model from the exponential model (100% cases $p\text{-value}<0.05$), and
270 the log-normal model (90% cases $p\text{-value}<0.05$).

271 The global mean of the power-law exponent α is 1.967 and the bootstrapped 95% confidence interval is
272 1.964 - 1.970. The global values for each threshold are different, because their confidence intervals do not
273 overlap, and their range goes from 1.90 to 2.01 (Table S1). Analyzing the biggest regions (Figure 1, Table
274 S2) the northern hemisphere regions (EUAS1 & NA1) have similar values of α (1.97, 1.98), pantropical areas

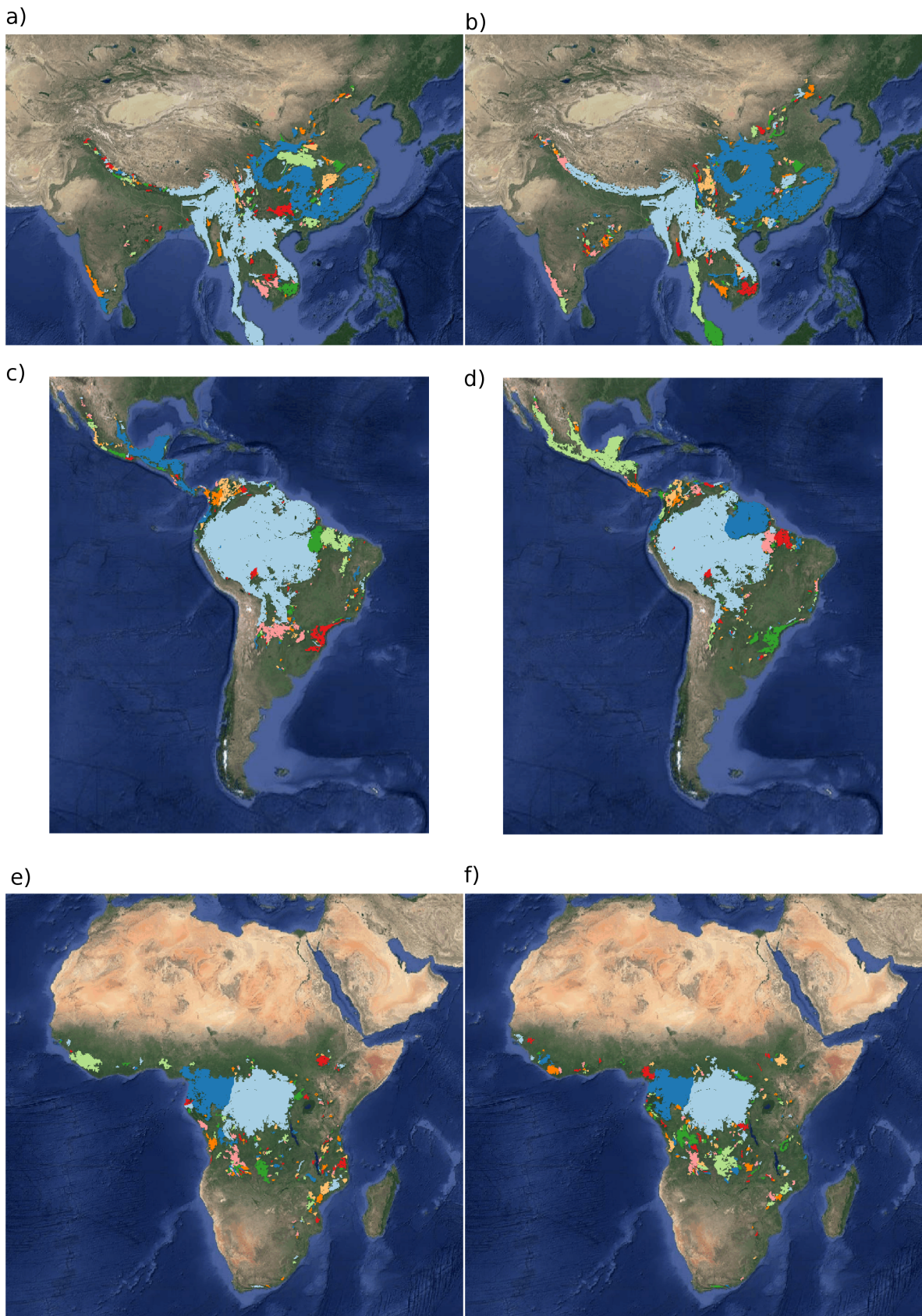


Figure 1: Forest patch distributions for continental regions for the years 2000 and 2014. The images are the 200 biggest patches, shown at a coarse pixel scale of 2.5 km. The regions are: a) & b) southeast Asia; c) & d) South America subtropical and tropical and e) & f) Africa mainland, for the years 2000 and 2014 respectively. The color palette was chosen to discriminate different patches and does not represent patch size.

275 have different α with greatest values for South America (SAST1, 2.01) and in descending order Africa (AF1,
 276 1.946) and Southeast Asia (SEAS1, 1.895). With greater α the fluctuations of patch sizes are lower and vice
 277 versa (Newman 2005).

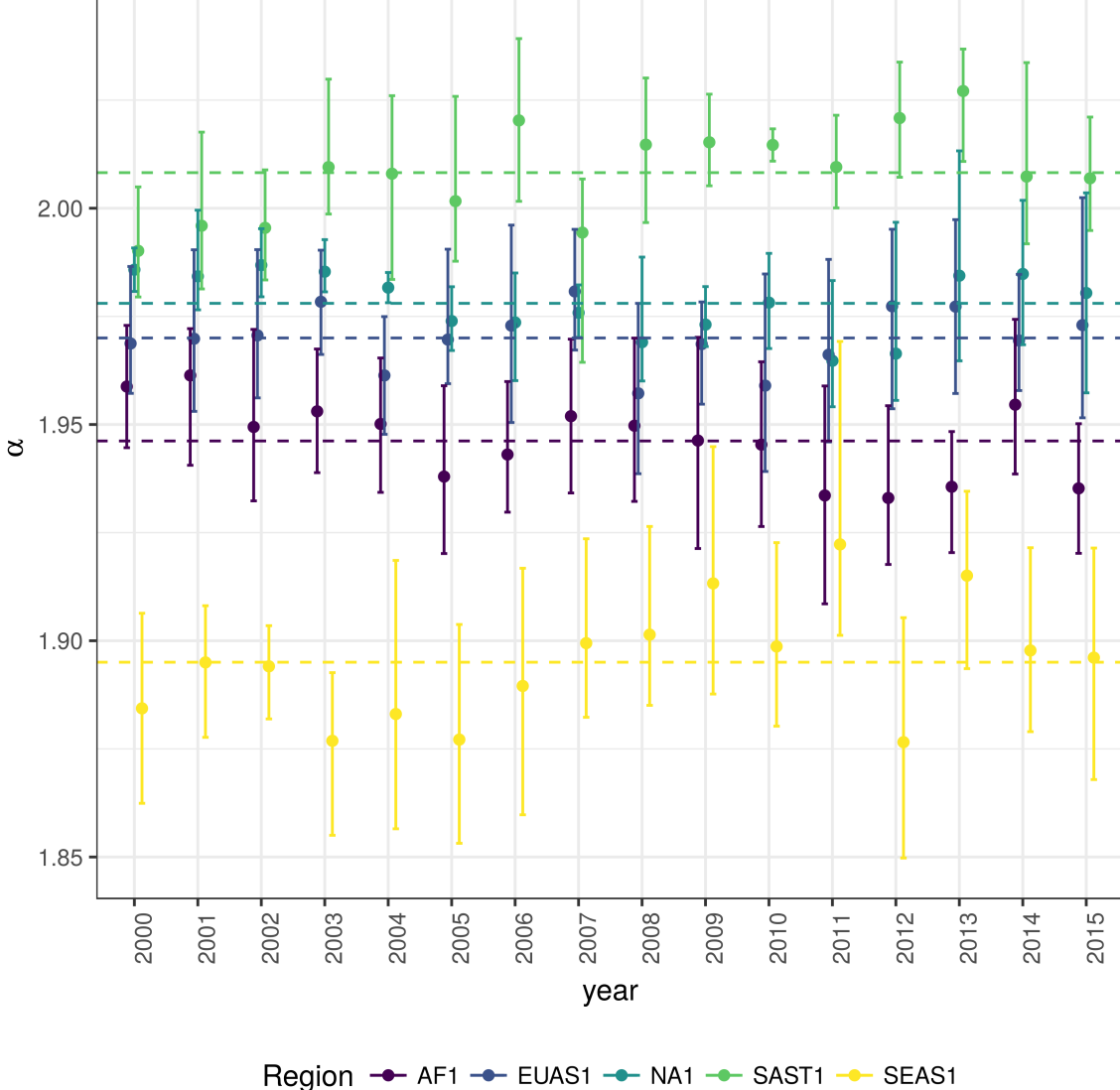


Figure 2: Power law exponents (α) of forest patch distributions for regions with total forest area $> 10^7$ km 2 . Dashed horizontal lines are the means by region, with 95% confidence interval error bars estimated by bootstrap resampling. The regions are AF1: Africa mainland, EUAS1: Eurasia mainland, NA1: North America mainland, SAST1: South America subtropical and tropical, SEAS1: Southeast Asia mainland.

278 We calculated the total areas of forest and the largest patch S_{max} by year for different thresholds, and as
 279 expected these two values increase for smaller thresholds (Table S3). We expect fewer variations in the
 280 largest patch relative to total forest area RS_{max} (Figure S9); in ten cases it stayed near or higher than 60%
 281 (EUAS2, NA5, OC2, OC3, OC4, OC5, OC6, OC8, SAST1, SAT1) over the 25-35 range or more. In four

282 cases it stayed around 40% or less, at least over the 25-30% range (AF1, EUAS3, OC1, SAST2), and in six
283 cases there is a crossover from more than 60% to around 40% or less (AF2, EUAS1, NA1, OC7, SEAS1,
284 SEAS2). This confirms the criteria of using the most conservative threshold value of 40% to interpret RS_{max}
285 with regard to the fragmentation state of the forest. The frequency of RS_{max} showed bimodality (Figure
286 S10) and the dip test rejected unimodality ($D = 0.0416$, p -value = 0.0003), which also implies that RS_{max}
287 is a good index to study the fragmentation state of the forest.

288 The RS_{max} for regions with more than 10^7 km 2 of forest is shown in figure 3. South America tropical and
289 subtropical (SAST1) is the only region with an average close to 60%, the other regions are below 30%. Eurasia
290 mainland (EUAS1) has the lowest value near 20%. For regions with less total forest area (Figure S10, Table
291 S3), Great Britain (EUAS3) has the lowest proportion less than 5%, Java (OC7) and Cuba (SAST2) are
292 under 25%, while other regions such as New Guinea (OC2), Malaysia/Kalimantan (OC3), Sumatra (OC4),
293 Sulawesi (OC5) and South New Zealand (OC6) have a very high proportion (75% or more). Philippines
294 (SEAS2) seems to be a very interesting case because it seems to be under 30% until the year 2007, fluctuates
295 around 30% in years 2008-2010, then jumps near 60% in 2011-2013 and then falls again to 30%, this seems
296 an example of a transition from a fragmented state to a unfragmented one (figure S11).

297 We analyzed the distributions of fluctuations of the largest patch relative to total forest area ΔRS_{max} and
298 the fluctuations of the largest patch ΔS_{max} . Although the Akaike criteria identified different distributions
299 as the best, in most cases the Likelihood ratio test was not significant and we are not able, from these data,
300 to determine with confidence which is the best distribution. In only one case was the distribution selected
301 by the Akaike criteria confirmed as the correct model for relative and absolute fluctuations (Table S4).

302 The animations of the two largest patches (see supplementary data, largest patch gif animations) qualitatively
303 shows the nature of fluctuations and if the state of the forest is connected or not. If the largest patch is
304 always the same patch over time, the forest is probably not fragmented; this happens for regions with RS_{max}
305 of more than 40% such as AF2 (Madagascar), EUAS2 (Japan), NA5 (Newfoundland) and OC3 (Malaysia).
306 In regions with RS_{max} between 40% and 30% the identity of the largest patch could change or stay the same
307 in time. For OC7 (Java) the largest patch changes and for AF1 (Africa mainland) it stays the same. Only for
308 EUAS1 (Eurasia mainland) did we observe that the two largest patches are always the same, implying that
309 this region is probably composed of two independent domains and should be sub-divided in future studies.
310 The regions with RS_{max} less than 25% included SAST2 (Cuba) and EUAS3 (Great Britain); in these cases
311 the always-changing largest patch reflects their fragmented state. In the case of SEAS2 (Philippines) a
312 transition is observed, with the identity of the largest patch first variable, and then constant after 2010.

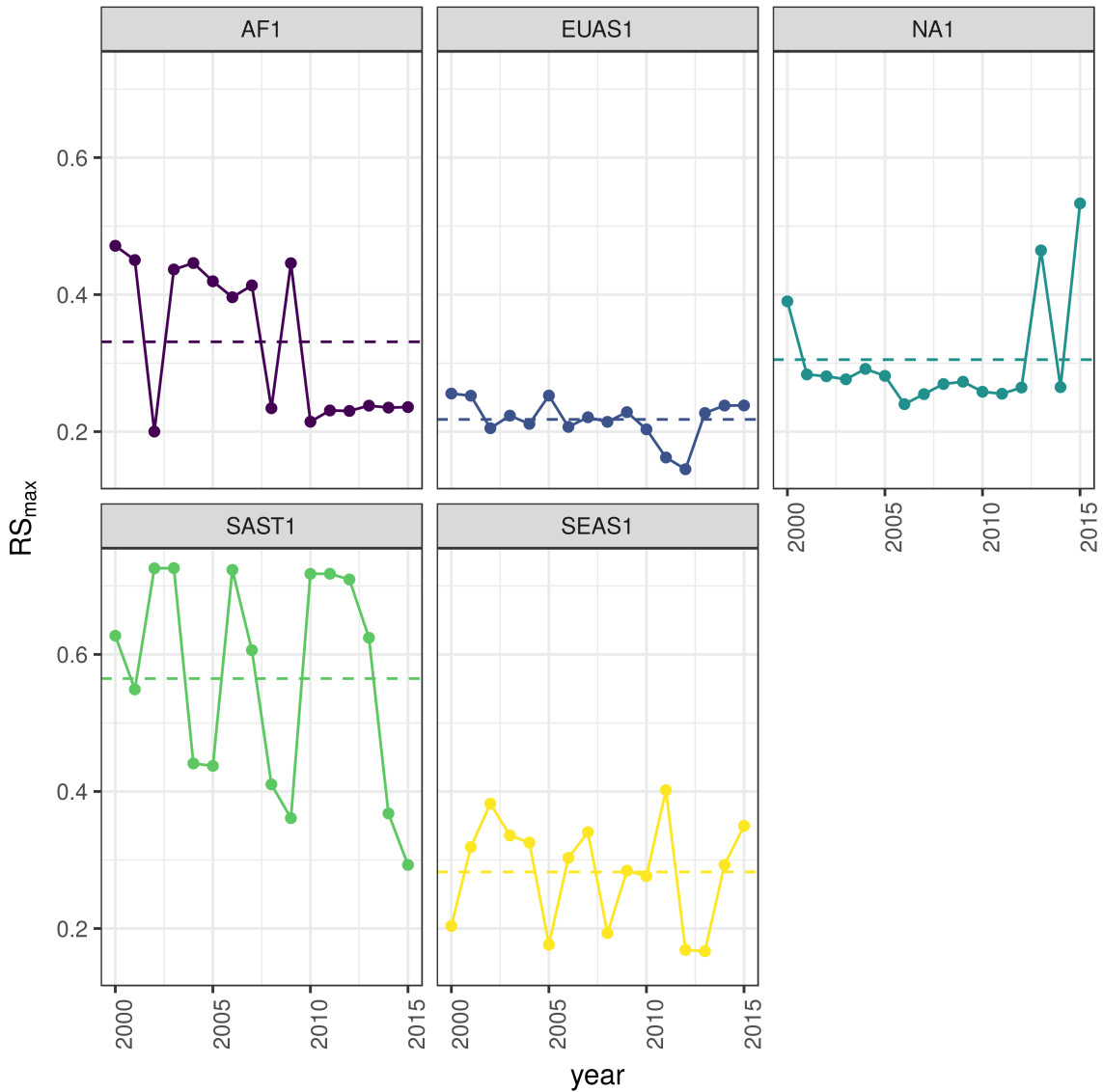


Figure 3: Largest patch proportion relative to total forest area RS_{max} , for regions with total forest area $> 10^7 \text{ km}^2$. We show here the RS_{max} calculated using a threshold of 40% of forest in each pixel to determine patches. Dashed lines are averages across time. The regions are AF1: Africa mainland, EUAS1: Eurasia mainland, NA1: North America mainland, SAST1: South America tropical and subtropical, SEAS1: Southeast Asia mainland.

313 The results of quantile regressions are almost identical for ΔRS_{max} and ΔS_{max} (table S5). Among the biggest
314 regions, Africa (AF1) has a similar pattern across thresholds but only the 30% threshold is significant; the
315 upper and lower quantiles have significant negative slopes, but the lower quantile slope is lower, implying
316 that negative fluctuations and variance are increasing (Figure 4). Eurasia mainland (EUAS1) has significant
317 slopes at 20%, 30% and 40% thresholds but the patterns are different at 20% variance is decreasing, at 30%
318 and 40% only is increasing. Thus the variation of the most dense portion of the largest patch is increasing
319 within a limited range. North America mainland (NA1) exhibits the same pattern at 20%, 25% and 30%
320 thresholds: a significant lower quantile with positive slope, implying decreasing variance. South America
321 tropical and subtropical (SAST1) have significant lower quantile with a negative slope at 25% and 30%
322 thresholds indicating an increase in variance. SEAS1 has an upper quantile with positive slope significant
323 for 25% threshold, also indicating an increasing variance. The other regions, with forest area smaller than
324 10^7 km^2 are shown in figure S11 and table S5. Philippines (SEAS2) is an interesting case: the slopes of lower
325 quantiles are positive for thresholds 20% and 25%, and the upper quantile slopes are positive for thresholds
326 30% and 40%; thus variance is decreasing at 20%-25% and increasing at 30%-40%.

327 The conditions that indicate that a region is near a critical fragmentation threshold are that patch size
328 distributions follow a power law; variance of ΔRS_{max} is increasing in time; and skewness is negative. All
329 these conditions must happen at the same time at least for one threshold. When the threshold is higher more
330 dense regions of the forest are at risk. This happens for Africa mainland (AF1), Eurasia mainland(EUAS1),
331 Japan (EUAS2), Australia mainland (OC1), Malaysia/Kalimantan (OC3), Sumatra (OC4), South America
332 tropical & subtropical (SAST1), Cuba (SAST2), Southeast Asia, Mainland (SEAS1).

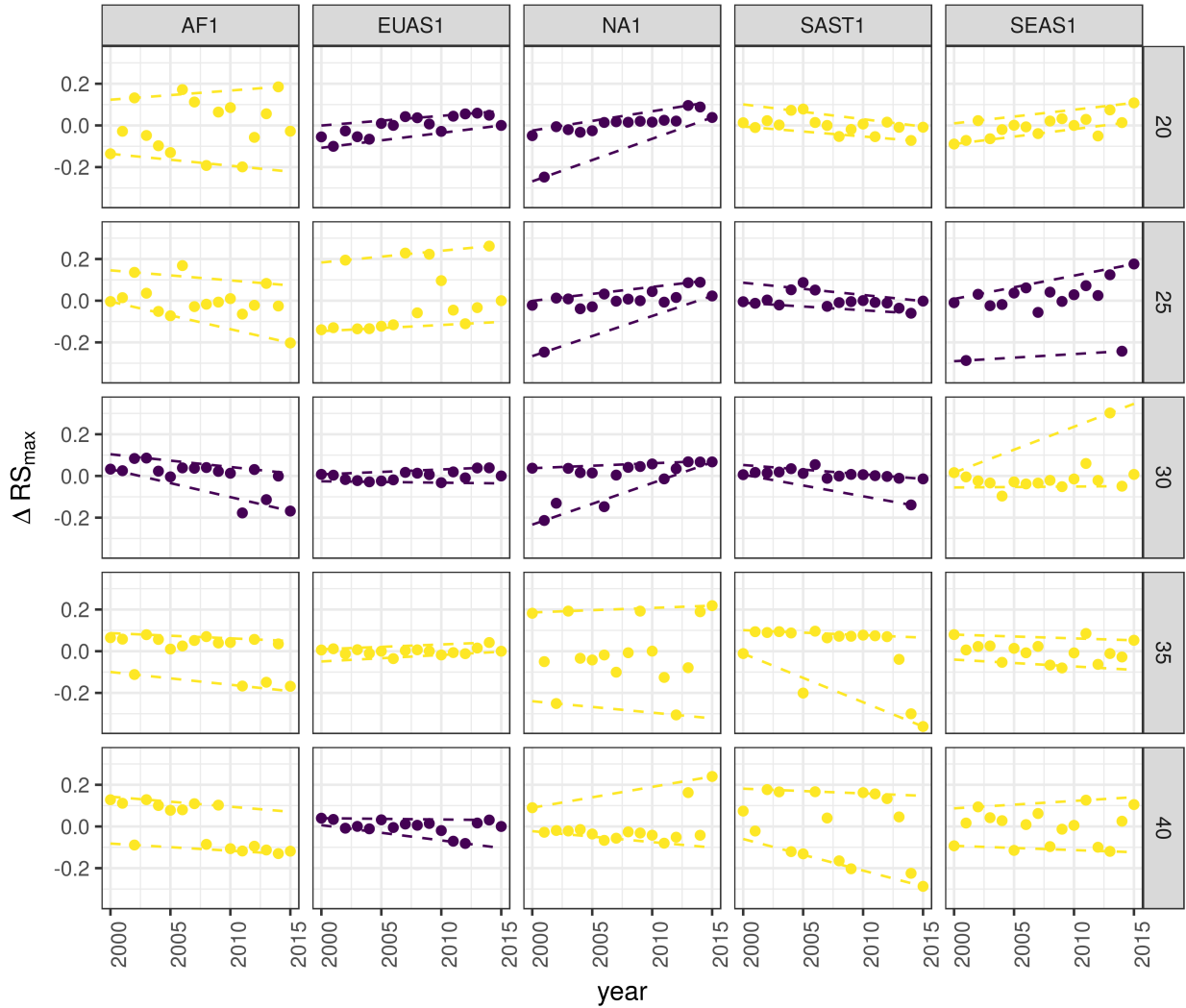


Figure 4: Largest patch fluctuations for regions with total forest area $> 10^7 \text{ km}^2$ across years. The patch sizes are relative to the total forest area of the same year. Dashed lines are 90% and 10% quantile regressions, to show if fluctuations were increasing; purple (dark) panels have significant slopes. The regions are AF1: Africa mainland, EUAS1: Eurasia mainland, NA1: North America mainland, SAST1: South America tropical and subtropical, SEAS1: Southeast Asia mainland.

Table 1: Regions and indicators of closeness to a critical fragmentation point. Where: RS_{max} is the largest patch divided by the total forest area; Threshold is the value used to calculate patches from the MODIS VCF pixels; ΔRS_{max} are the fluctuations of RS_{max} around the mean and the increase or decrease in the variance was estimated using quantile regressions; skewness was calculated for RS_{max} . NS means the results were non-significant. The conditions that determine the closeness to a fragmentation point are: increasing variance of ΔRS_{max} and negative skewness. RS_{max} indicates if the forest is unfragmented (>0.6) or fragmented (<0.3).

Region	Description	RS_{max}	Threshold	Variance of ΔRS_{max}	Skewness
AF1	Africa mainland	0.33	30	Increase	-1.4653
AF2	Madagascar	0.48	20	Increase	0.7226
EUAS1	Eurasia, mainland	0.22	20	Decrease	-0.4814
EUAS1			30	Increase	0.3113
EUAS1			40	Increase	-1.2790
EUAS2	Japan	0.94	35	Increase	-0.3913
EUAS2			40	Increase	-0.5030
EUAS3	Great Britain	0.03	40	NS	
NA1	North America, mainland	0.31	20	Decrease	-2.2895
NA1			25	Decrease	-2.4465
NA1			30	Decrease	-1.6340
NA5	Newfoundland	0.54	40	NS	
OC1	Australia, Mainland	0.36	30	Increase	0.0920
OC1			35	Increase	-0.8033
OC2	New Guinea	0.96	25	Decrease	-0.1003
OC2			30	Decrease	0.1214
OC2			35	Decrease	-0.0124
OC3	Malaysia/Kalimantan	0.92	35	Increase	-1.0147
OC3			40	Increase	-1.5649
OC4	Sumatra	0.84	20	Increase	-1.3846
OC4			25	Increase	-0.5887
OC4			30	Increase	-1.4226
OC5	Sulawesi	0.82	40	NS	
OC6	New Zealand South Island	0.75	40	Increase	0.3553
OC7	Java	0.16	40	NS	
OC8	New Zealand North Island	0.64	40	NS	
SAST1	South America, Tropical and Subtropical forest	0.56	25	Increase	1.0519
SAST1			30	Increase	-2.7216
SAST2	Cuba	0.15	20	Increase	0.5049
SAST2			25	Increase	1.7263
SAST2			30	Increase	0.1665
SAST2			40	Increase	-0.5401
SAT1	South America, Temperate forest	0.54	25	Decrease	0.1483
SAT1			30	Decrease	-1.6059
SAT1			35	Decrease	-1.3809
SEAS1	Southeast Asia, Mainland	0.28	25	Increase	-1.3328
SEAS2	Philippines	0.33	20	Decrease	-1.6373
SEAS2			25	Decrease	-0.6648
SEAS2			30	Increase	0.1517

Region	Description	RS_{max}	Threshold	Variance of ΔRS_{max}	Skewness
SEAS2			40	Increase	1.5996

333 Discussion

334 We found that the forest patch distribution of all regions of the world, spanning tropical rainforests, boreal
 335 and temperate forests, followed power laws spanning seven orders of magnitude. Power laws have previously
 336 been found for several kinds of vegetation, but never at global scales as in this study. Moreover, the range
 337 of the estimated power law exponents is relatively narrow (1.90 - 2.01), even though we tested a variety
 338 of different thresholds levels. This suggests the existence of one unifying mechanism, or perhaps different
 339 mechanisms that act in the same way in different regions, affecting forest spatial structure and dynamics.

340 Several mechanisms have been proposed for the emergence of power laws in forests. The first is related self
 341 organized criticality (SOC), when the system is driven by its internal dynamics to a critical state; this has
 342 been suggested mainly for fire-driven forests (Zinck & Grimm 2009; Hantson *et al.* 2015). Real ecosystems
 343 do not seem to meet the requirements of SOC dynamics (Pueyo *et al.* 2010; McKenzie & Kennedy 2012),
 344 however, because they have both endogenous and exogenous controls, are non-homogeneous, and do not
 345 have a separation of time scales (Solé *et al.* 2002; Solé & Bascompte 2006). A second possible mechanism,
 346 suggested by Pueyo *et al.* (2010), is isotropic percolation: when a system is near the critical point, the power
 347 law structures arise. This is equivalent to the random forest model that we explained previously, and requires
 348 the tuning of an external environmental condition to carry the system to this point. We did not expect forest
 349 growth to be a random process at local scales, but it is possible that combinations of factors cancel out to
 350 produce seemingly random forest dynamics at large scales. This has been suggested as a mechanism for the
 351 observed power laws of global tropical forest at year 2000 (Taubert *et al.* 2018). In this case we should have
 352 observed power laws in a limited set of situations that coincide with a critical point, but instead we observed
 353 pervasive power law distributions. Thus isotropic percolation does not seem likely to be the mechanism that
 354 produces the observed distributions. A third possible mechanism is facilitation (Manor & Shnerb 2008; Irvine
 355 *et al.* 2016): a patch surrounded by forest will have a smaller probability of being deforested or degraded
 356 than an isolated patch. The model of Scanlon *et al.* (2007) showed an $\alpha = 1.34$ which is different from our
 357 results (1.90 - 2.01 range). Another model but with three states (tree/non-tree/degraded), including local
 358 facilitation and grazing, was also used to obtain power laws patch distributions without external tuning, and
 359 exhibited deviations from power laws at high grazing pressures (Kéfi *et al.* 2007). The values of the power
 360 law exponent α obtained for this model are dependent on the intensity of facilitation: when facilitation is

more intense the exponent is higher, but the maximal values they obtained are still lower than the ones we observed. The interesting point is that the value of the exponent is dependent on the parameters, and thus the observed α might be obtained with some parameter combination.

The existence of possible critical transitions in forests, mainly in neotropical forest to savanna, is a matter of intense investigation, with the transitions generally thought to be first order or discontinuous transitions. Here, however, we found power laws in forest patch distributions, implying (i.e., a necessary but not a sufficient condition) a second order or continuous transition. A power law patch distribution can be indicative of a critical transition if it is present in a narrow range of conditions; conversely, if it is not found, the existence of a critical transition cannot be discarded. New research (Villa Martín *et al.* 2014, 2015) has suggested that first order transitions do not even exist when the system is (i) spatially heterogeneous and (ii) exhibits internal and external stochastic fluctuations, as in forests. Thus the application of indices based on second order transitions seems to be justified.

It has been suggested that a combination of spatial and temporal indicators could more reliably detect critical transitions (Kéfi *et al.* 2014). In this study, we combined five criteria to evaluate the closeness of the system to a fragmentation threshold. Two of them were spatial: the forest patch size distribution, and the proportion of the largest patch relative to total forest area RS_{max} . The other three were the distribution of temporal fluctuations in the largest patch size, the trend in the variance, and the skewness of the fluctuations. One of them: the distribution of temporal fluctuations ΔRS_{max} can not be applied with our temporal resolution due to the difficulties of fitting and comparing heavy tailed distributions. The combination of the remaining four gives us an increased degree of confidence about the system being close to a critical transition.

Monitoring the biggest patches using RS_{max} is also important regardless of the existence or not of critical transitions. RS_{max} is relative to total forest area thus it could be used to compare regions with a different extension of forests and as the total area of forest also changes with different environmental conditions, e.g. this could be used to compare forest from different latitudes. Moreover, the areas covered by S_{max} across regions contain most of the intact forest landscapes defined by Potapov *et al.* (2008b), and thus RS_{max} is a relatively simple way to evaluate the risk in these areas.

This analysis is at scale of continents so it is in fact a macrosystems analysis (Heffernan *et al.* 2014), in which it is important to link local processes with resulting larger-scale (here, continental) patterns. Here, we identified macro-scale dynamical patterns that deserve attention. To link these patterns across scales requires a substantial amount of investigation, probably performing the same analysis for smaller regions that identify more clearly which kind of forest and processes are locally involved. We know that the same procedure could

392 be applied to local scales because the patch distributions are power laws; power law distributions are self-
393 similar, or invariant to scale changes. Thus unless power law distribution are broken we could apply the
394 same methodology to more local scales.

395 South America tropical and subtropical (SAST1), Southeast Asia mainland (SEAS1) and Africa mainland
396 (AF1) met all criteria at least for one threshold; these regions generally experience the biggest rates of
397 deforestation with a significant increase in loss of forest (Hansen *et al.* 2013). From our point of view the
398 most critical region is Southeast Asia, because the proportion of the largest patch relative to total forest
399 area RS_{max} was 28%. This suggests that Southeast Asia's forests are the most fragmented, and thus its
400 flora and fauna the most endangered. Due to the criteria we adopted to define regions, we could not detect
401 the effect of conservation policies applied at a country level, e.g. the Natural Forest Conservation Program
402 in China, which has produced an 1.6% increase in forest cover and net primary productivity over the last 20
403 years (Viña *et al.* 2016). Indonesia and Malaysia (OC3) both are countries with hight deforestation rates
404 (Hansen *et al.* 2013); Sumatra (OC4) is the biggest island of Indonesia and where most deforestation occurs.
405 Both regions show a high RS_{max} greater than 60%, and thus the forest is in an unfragmented state, but
406 they met all other criteria, meaning that they are approaching a transition if the actual deforestation rates
407 continue. At present our indices are qualitative but we expect to develop them in a more quantitative way
408 to predict how many years would be needed to complete a critical transition if actual forest loss rates are
409 maintained.

410 The Eurasian mainland region (EUAS1) is an extensive area with mainly temperate and boreal forest, and a
411 combination of forest loss due to fire (Potapov *et al.* 2008a) and forestry. The biggest country is Russia that
412 experienced the biggest rate of forest loss of all countries, but here in the zone of coniferous forest the the
413 largest gain is observed due to agricultural abandonment (Prishchepov *et al.* 2013). The loss is maximum
414 at the most dense areas of forest (Hansen *et al.* 2013, Table S3), this coincides with our analysis that detect
415 an increasing risk at denser forest. This region also has a relatively low RS_{max} that means is probably near
416 a fragmented state. A region that is similar in forest composition to EAUS1 is North America (NA1); the
417 two main countries involved, United States and Canada, have forest dynamics mainly influenced by fire and
418 forestry, with both regions are extensively managed for industrial wood production. North America has a
419 higher RS_{max} than Eurasia and a positive skewness that excludes it from being near a critical transition. A
420 possible explanation of this is that in Russia after the collapse of the Soviet Union harvest was lower due to
421 agricultural abandonment but illegal overharvesting of high valued stands has increased in recent decades
422 (Gauthier *et al.* 2015).

423 The analysis of RS_{max} reveals that the island of Philippines (SEAS2) seems to be an example of a critical

424 transition from an unconnected to a connected state, i.e. from a state with high fluctuations and low RS_{max}
425 to a state with low fluctuations and high RS_{max} . If we observe this pattern backwards in time, the decrease
426 in variance increases, and negative skewness is constant, and thus the region exhibits the criteria of a critical
427 transition (Table 1, Figure S12). The actual pattern of transition to an unfragmented state could be the
428 result of an active intervention of the government promoting conservation and rehabilitation of protected
429 areas, ban of logging old-growth forest, reforestation of barren areas, community-based forestry activities,
430 and sustainable forest management in the country's production forest (Lasco *et al.* 2008). This confirms that
431 the early warning indicators proposed here work in the correct direction. An important caveat is that the
432 MODIS dataset does not detect if native forest is replaced by agroindustrial tree plantations like oil palms,
433 that are among the main drivers of deforestation in this area (Malhi *et al.* 2014). To improve the estimation
434 of forest patches, data sets as the MODIS cropland probability and others about land use, protected areas,
435 forest type, should be incorporated (Hansen *et al.* 2014; Sexton *et al.* 2015).

436 Deforestation and fragmentation are closely related. At low levels of habitat reduction species population
437 will decline proportionally; this can happen even when the habitat fragments retain connectivity. As habitat
438 reduction continues, the critical threshold is approached and connectivity will have large fluctuations (Brook
439 *et al.* 2013). This could trigger several negative synergistic effects: population fluctuations and the possibility
440 of extinctions will rise, increasing patch isolation and decreasing connectivity (Brook *et al.* 2013). This
441 positive feedback mechanism will be enhanced when the fragmentation threshold is reached, resulting in the
442 loss of most habitat specialist species at a landscape scale (Pardini *et al.* 2010). Some authors have argued
443 that since species have heterogeneous responses to habitat loss and fragmentation, and biotic dispersal is
444 limited, the importance of thresholds is restricted to local scales or even that its existence is questionable
445 (Brook *et al.* 2013). Fragmentation is by definition a local process that at some point produces emergent
446 phenomena over the entire landscape, even if the area considered is infinite (Oborny *et al.* 2005). In
447 addition, after a region's fragmentation threshold connectivity decreases, there is still a large and internally
448 well connected patch that can maintain sensitive species (Martensen *et al.* 2012). What is the time needed
449 for these large patches to become fragmented, and pose a real danger of extinction to a myriad of sensitive
450 species? If a forest is already in a fragmented state, a second critical transition from forest to non-forest
451 could happen: the desertification transition (Corrado *et al.* 2014). Considering the actual trends of habitat
452 loss, and studying the dynamics of non-forest patches—instead of the forest patches as we did here—the risk
453 of this kind of transition could be estimated. The simple models proposed previously could also be used to
454 estimate if these thresholds are likely to be continuous and reversible or discontinuous and often irreversible
455 (Weissmann & Shnerb 2016), and the degree of protection (e.g. using the set-asides strategy Banks-Leite *et*

456 *al.* (2014)) that would be necessary to stop this trend.

457 The effectiveness of landscape management is related to the degree of fragmentation, and the criteria to direct
458 reforestation efforts could be focused on regions near a transition (Oborny *et al.* 2007). Regions that are in
459 an unconnected state require large efforts to recover a connected state, but regions that are near a transition
460 could be easily pushed to a connected state; feedbacks due to facilitation mechanisms might help to maintain
461 this state. Crossing the fragmentation critical point in forests could have negative effects on biodiversity and
462 ecosystem services (Haddad *et al.* 2015), but it could also produce feedback loops at different levels of the
463 biological hierarchy. This means that a critical transition produced at a continental scale could have effects
464 at the level of communities, food webs, populations, phenotypes and genotypes (Barnosky *et al.* 2012). All
465 these effects interact with climate change, thus there is a potential production of cascading effects that could
466 lead to an abrupt climate change with potentially large ecological and economic impact (Alley *et al.* 2003).

467 Therefore, even if critical thresholds are reached only in some forest regions at a continental scale, a cascading
468 effect with global consequences could still be produced (Reyer *et al.* 2015). The risk of such event will be
469 higher if the dynamics of separate continental regions are coupled (Lenton & Williams 2013). At least
470 three of the regions defined here are considered tipping elements of the earth climate system that could be
471 triggered during this century (Lenton *et al.* 2008). These were defined as policy relevant tipping elements
472 so that political decisions could determine whether the critical value is reached or not. Thus using the
473 criteria proposed here could be used as a more sensitive system to evaluate the closeness of a tipping point
474 at a continental scale, but the same criteria could also be uses to evaluate local problems at smaller areas.
475 Further improvements will produce quantitative predictions about the temporal horizon where these critical
476 transitions could produce significant changes in the studied systems.

477 Supporting information

478 Appendix

479 *Table S1:* Mean power-law exponent and Bootstrapped 95% confidence intervals by threshold.

480 *Table S2:* Mean power-law exponent and Bootstrapped 95% confidence intervals across thresholds by region
481 and year.

482 *Table S3:* Mean total patch area; largest patch S_{max} in km²; largest patch proportional to total patch area
483 RS_{max} and 95% bootstrapped confidence interval of RS_{max} , by region and thresholds, averaged across years

484 *Table S4:* Model selection for distributions of fluctuation of largest patch ΔS_{max} and largest patch relative

485 to total forest area ΔRS_{max} .

486 *Table S5*: Quantil regressions of the fluctuations of the largest patch vs year, for 10% and 90% quantils at
487 different pixel thresholds.

488 *Table S6*: Unbiased estimation of Skewness of fluctuations of the largest patch ΔS_{max} and fluctuations
489 relative to total forest area ΔRS_{max} .

490 *Figure S1*: Regions for Africa: Mainland (AF1), Madagascar (AF2).

491 *Figure S2*: Regions for Eurasia: Mainland (EUAS1), Japan (EUAS2), Great Britain (EUAS3).

492 *Figure S3*: Regions for North America: Mainland (NA1), Newfoundland (NA5).

493 *Figure S4*: Regions for Australia and islands: Australia mainland (OC1), New Guinea (OC2),
494 Malaysia/Kalimantan (OC3), Sumatra (OC4), Sulawesi (OC5), New Zealand south island (OC6),
495 Java (OC7), New Zealand north island (OC8).

496 *Figure S5*: Regions for South America: Tropical and subtropical forest up to Mexico (SAST1), Cuba
497 (SAST2), South America Temperate forest (SAT1).

498 *Figure S6*: Regions for Southeast Asia: Mainland (SEAS1), Philippines (SEAS2).

499 *Figure S7*: Proportion of best models selected for patch size distributions using the Akaike criterion.

500 *Figure S8*: Power law exponents for forest patch distributions by year for all regions.

501 *Figure S9*: Average largest patch relative to total forest area RS_{max} by threshold, for all regions.

502 *Figure S10*: Frequency distribution of Largest patch proportion relative to total forest area RS_{max} calculated
503 using a threshold of 40%.

504 *Figure S11*: Largest patch relative to total forest area RS_{max} by year at 40% threshold, for regions with
505 total forest area less than 10^7 km^2 .

506 *Figure S12*: Fluctuations of largest patch relative to total forest area RS_{max} for regions with total forest
507 area less than 10^7 km^2 by year and threshold.

508 Data Accessibility

509 The MODIS VCF product is freely available from NASA at <https://search.earthdata.nasa.gov/>. Csv text file
510 with model fits for patch size distribution, and model selection for all the regions; Gif Animations of a forest

511 model percolation; Gif animations of largest patches; patch size files for all years and regions used here; and all
512 the R, Python and Matlab scripts are available at figshare <http://dx.doi.org/10.6084/m9.figshare.4263905>.

513 **Acknowledgments**

514 LAS and SRD are grateful to the National University of General Sarmiento for financial support. We want to
515 thank to Jordi Bascompte, Nara Guisoni, Fernando Momo, and two anonymous reviewers for their comments
516 and discussions that greatly improved the manuscript. This work was partially supported by a grant from
517 CONICET (PIO 144-20140100035-CO).

518 **References**

- 519 Alley, R.B., Marotzke, J., Nordhaus, W.D., Overpeck, J.T., Peteet, D.M. & Pielke, R.A. *et al.* (2003).
520 Abrupt Climate Change. *Science*, 299, 2005–2010.
- 521 Allington, G.R.H. & Valone, T.J. (2010). Reversal of desertification: The role of physical and chemical soil
522 properties. *Journal of Arid Environments*, 74, 973–977.
- 523 Alstott, J., Bullmore, E. & Plenz, D. (2014). powerlaw: A Python Package for Analysis of Heavy-Tailed
524 Distributions. *PLOS ONE*, 9, e85777.
- 525 Angelsen, A. (2010). Policies for reduced deforestation and their impact on agricultural production. *Pro-*
526 *ceedings of the National Academy of Sciences*, 107, 19639–19644.
- 527 Banks-Leite, C., Pardini, R., Tambosi, L.R., Pearse, W.D., Bueno, A.A. & Bruscagin, R.T. *et al.* (2014).
528 Using ecological thresholds to evaluate the costs and benefits of set-asides in a biodiversity hotspot. *Science*,
529 345, 1041–1045.
- 530 Barnosky, A.D., Hadly, E.A., Bascompte, J., Berlow, E.L., Brown, J.H. & Fortelius, M. *et al.* (2012).
531 Approaching a state shift in Earth’s biosphere. *Nature*, 486, 52–58.
- 532 Bascompte, J. & Solé, R.V. (1996). Habitat fragmentation and extinction threholds in spatially explicit
533 models. *Journal of Animal Ecology*, 65, 465–473.
- 534 Bazant, M.Z. (2000). Largest cluster in subcritical percolation. *Physical Review E*, 62, 1660–1669.
- 535 Belward, A.S. (1996). *The IGBP-DIS Global 1 Km Land Cover Data Set “DISCover”: Proposal and*
536 *Implementation Plans : Report of the Land Recover Working Group of IGBP-DIS*. IGBP-dis working paper.

- 537 IGBP-DIS Office.
- 538 Benedetti-Cecchi, L., Tamburello, L., Maggi, E. & Bulleri, F. (2015). Experimental Perturbations Modify
539 the Performance of Early Warning Indicators of Regime Shift. *Current biology*, 25, 1867–1872.
- 540 Bestelmeyer, B.T., Duniway, M.C., James, D.K., Burkett, L.M. & Havstad, K.M. (2013). A test of critical
541 thresholds and their indicators in a desertification-prone ecosystem: more resilience than we thought. *Ecology*
542 *Letters*, 16, 339–345.
- 543 Bestelmeyer, B.T., Ellison, A.M., Fraser, W.R., Gorman, K.B., Holbrook, S.J. & Laney, C.M. *et al.* (2011).
544 Analysis of abrupt transitions in ecological systems. *Ecosphere*, 2, 129.
- 545 Boettiger, C. & Hastings, A. (2012). Quantifying limits to detection of early warning for critical transitions.
546 *Journal of The Royal Society Interface*, 9, 2527–2539.
- 547 Bonan, G.B. (2008). Forests and Climate Change: Forcings, Feedbacks, and the Climate Benefits of Forests.
548 *Science*, 320, 1444–1449.
- 549 Botet, R. & Ploszajczak, M. (2004). Correlations in Finite Systems and Their Universal Scaling Properties.
550 In: *Nonequilibrium physics at short time scales: Formation of correlations* (ed. Morawetz, K.). Springer-
551 Verlag, Berlin Heidelberg, pp. 445–466.
- 552 Brook, B.W., Ellis, E.C., Perring, M.P., Mackay, A.W. & Blomqvist, L. (2013). Does the terrestrial biosphere
553 have planetary tipping points? *Trends in Ecology & Evolution*.
- 554 Burnham, K. & Anderson, D.R. (2002). *Model selection and multi-model inference: A practical information-
555 theoretic approach*. 2nd. edn. Springer-Verlag, New York.
- 556 Canfield, D.E., Glazer, A.N. & Falkowski, P.G. (2010). The Evolution and Future of Earth's Nitrogen Cycle.
557 *Science*, 330, 192–196.
- 558 Carpenter, S.R., Cole, J.J., Pace, M.L., Batt, R., Brock, W.A. & Cline, T. *et al.* (2011). Early Warnings of
559 Regime Shifts: A Whole-Ecosystem Experiment. *Science*, 332, 1079–1082.
- 560 Clauset, A., Shalizi, C. & Newman, M. (2009). Power-Law Distributions in Empirical Data. *SIAM Review*,
561 51, 661–703.
- 562 Corrado, R., Cherubini, A.M. & Pennetta, C. (2014). Early warning signals of desertification transitions in

- 563 semiarid ecosystems. *Physical Review E - Statistical, Nonlinear, and Soft Matter Physics*, 90, 62705.
- 564 Crawley, M.J. (2012). *The R Book*. 2nd. edn. Wiley, Hoboken, NJ, USA.
- 565 Crowther, T.W., Glick, H.B., Covey, K.R., Bettigole, C., Maynard, D.S. & Thomas, S.M. *et al.* (2015).
- 566 Mapping tree density at a global scale. *Nature*, 525, 201–205.
- 567 Dai, L., Vorselen, D., Korolev, K.S. & Gore, J. (2012). Generic Indicators for Loss of Resilience Before a
568 Tipping Point Leading to Population Collapse. *Science*, 336, 1175–1177.
- 569 DiMiceli, C., Carroll, M., Sohlberg, R., Huang, C., Hansen, M. & Townshend, J. (2015). Annual Global
570 Automated MODIS Vegetation Continuous Fields (MOD44B) at 250 m Spatial Resolution for Data Years
571 Beginning Day 65, 2000 - 2014, Collection 051 Percent Tree Cover, University of Maryland, College Park,
572 MD, USA.
- 573 Drake, J.M. & Griffen, B.D. (2010). Early warning signals of extinction in deteriorating environments.
574 *Nature*, 467, 456–459.
- 575 Efron, B. & Tibshirani, R.J. (1994). *An Introduction to the Bootstrap*. Chapman & hall/crc monographs on
576 statistics & applied probability. Taylor & Francis, New York.
- 577 Filotas, E., Parrott, L., Burton, P.J., Chazdon, R.L., Coates, K.D. & Coll, L. *et al.* (2014). Viewing forests
578 through the lens of complex systems science. *Ecosphere*, 5, 1–23.
- 579 Foley, J.A., Ramankutty, N., Brauman, K.A., Cassidy, E.S., Gerber, J.S. & Johnston, M. *et al.* (2011).
580 Solutions for a cultivated planet. *Nature*, 478, 337–342.
- 581 Folke, C., Jansson, Å., Rockström, J., Olsson, P., Carpenter, S.R. & Iii, F.S.C. *et al.* (2011). Reconnecting
582 to the Biosphere. *AMBIO*, 40, 719–738.
- 583 Fung, T., O'Dwyer, J.P., Rahman, K.A., Fletcher, C.D. & Chisholm, R.A. (2016). Reproducing static and
584 dynamic biodiversity patterns in tropical forests: the critical role of environmental variance. *Ecology*, 97,
585 1207–1217.
- 586 Gardner, R.H. & Urban, D.L. (2007). Neutral models for testing landscape hypotheses. *Landscape Ecology*,
587 22, 15–29.
- 588 Gastner, M.T., Oborny, B., Zimmermann, D.K. & Pruessner, G. (2009). Transition from Connected to Frag-
589 mented Vegetation across an Environmental Gradient: Scaling Laws in Ecotone Geometry. *The American
590 Naturalist*, 174, E23–E39.
- 591 Gauthier, S., Bernier, P., Kuuluvainen, T., Shvidenko, A.Z. & Schepaschenko, D.G. (2015). Boreal forest

- 592 health and global change. *Science*, 349, 819 LP–822.
- 593 Gilman, S.E., Urban, M.C., Tewksbury, J., Gilchrist, G.W. & Holt, R.D. (2010). A framework for community
594 interactions under climate change. *Trends in Ecology & Evolution*, 25, 325–331.
- 595 Goldstein, M.L., Morris, S.A. & Yen, G.G. (2004). Problems with fitting to the power-law distribution. *The
596 European Physical Journal B - Condensed Matter and Complex Systems*, 41, 255–258.
- 597 Haddad, N.M., Brudvig, L.a., Clobert, J., Davies, K.F., Gonzalez, A. & Holt, R.D. *et al.* (2015). Habitat
598 fragmentation and its lasting impact on Earth’s ecosystems. *Science Advances*, 1, 1–9.
- 599 Hansen, M., Potapov, P., Margono, B., Stehman, S., Turubanova, S. & Tyukavina, A. (2014). Response to
600 Comment on “High-resolution global maps of 21st-century forest cover change”. *Science*, 344, 981.
- 601 Hansen, M.C., Potapov, P.V., Moore, R., Hancher, M., Turubanova, S.A. & Tyukavina, A. *et al.* (2013).
602 High-Resolution Global Maps of 21st-Century Forest Cover Change. *Science*, 342, 850–853.
- 603 Hantson, S., Pueyo, S. & Chuvieco, E. (2015). Global fire size distribution is driven by human impact and
604 climate. *Global Ecology and Biogeography*, 24, 77–86.
- 605 Harris, T.E. (1974). Contact interactions on a lattice. *The Annals of Probability*, 2, 969–988.
- 606 Hartigan, J.A. & Hartigan, P.M. (1985). The Dip Test of Unimodality. *The Annals of Statistics*, 13, 70–84.
- 607 Hastings, A. & Wysham, D.B. (2010). Regime shifts in ecological systems can occur with no warning. *Ecology
Letters*, 13, 464–472.
- 609 He, F. & Hubbell, S. (2003). Percolation Theory for the Distribution and Abundance of Species. *Physical
Review Letters*, 91, 198103.
- 611 Heffernan, J.B., Soranno, P.A., Angilletta, M.J., Buckley, L.B., Gruner, D.S. & Keitt, T.H. *et al.* (2014).
612 Macrosystems ecology: understanding ecological patterns and processes at continental scales. *Frontiers in
613 Ecology and the Environment*, 12, 5–14.
- 614 Hinrichsen, H. (2000). Non-equilibrium critical phenomena and phase transitions into absorbing states.
615 *Advances in Physics*, 49, 815–958.
- 616 Hirota, M., Holmgren, M., Nes, E.H.V. & Scheffer, M. (2011). Global Resilience of Tropical Forest and
617 Savanna to Critical Transitions. *Science*, 334, 232–235.
- 618 Irvine, M.A., Bull, J.C. & Keeling, M.J. (2016). Aggregation dynamics explain vegetation patch-size distri-

- 619 butions. *Theoretical Population Biology*, 108, 70–74.
- 620 Keitt, T.H., Urban, D.L. & Milne, B.T. (1997). Detecting critical scales in fragmented landscapes. *Conserv-
621 ation Ecology*, 1, 4.
- 622 Kéfi, S., Guttal, V., Brock, W.A., Carpenter, S.R., Ellison, A.M. & Livina, V.N. *et al.* (2014). Early
623 Warning Signals of Ecological Transitions: Methods for Spatial Patterns. *PLoS ONE*, 9, e92097.
- 624 Kéfi, S., Rietkerk, M., Alados, C.L., Pueyo, Y., Papanastasis, V.P. & ElAich, A. *et al.* (2007). Spatial
625 vegetation patterns and imminent desertification in Mediterranean arid ecosystems. *Nature*, 449, 213–217.
- 626 Kitzberger, T., Aráoz, E., Gowda, J.H., Mermoz, M. & Morales, J.M. (2012). Decreases in Fire Spread Prob-
627 ability with Forest Age Promotes Alternative Community States, Reduced Resilience to Climate Variability
628 and Large Fire Regime Shifts. *Ecosystems*, 15, 97–112.
- 629 Koenker, R. (2016). quantreg: Quantile Regression.
- 630 Lasco, R.D., Pulhin, F.B., Cruz, R.V.O., Pulhin, J.M., Roy, S.S.N. & Sanchez, P.A.J. (2008). Forest
631 responses to changing rainfall in the Philippines. In: *Climate change and vulnerability* (eds. Leary, N.,
632 Conde, C. & Kulkarni, J.). Earthscan, London, pp. 49–66.
- 633 Leibold, M.A. & Norberg, J. (2004). Biodiversity in metacommunities: Plankton as complex adaptive
634 systems? *Limnology and Oceanography*, 49, 1278–1289.
- 635 Lenton, T.M. & Williams, H.T.P. (2013). On the origin of planetary-scale tipping points. *Trends in Ecology
636 & Evolution*, 28, 380–382.
- 637 Lenton, T.M., Held, H., Kriegler, E., Hall, J.W., Lucht, W. & Rahmstorf, S. *et al.* (2008). Tipping elements
638 in the Earth's climate system. *Proceedings of the National Academy of Sciences*, 105, 1786–1793.
- 639 Limpert, E., Stahel, W.A. & Abbt, M. (2001). Log-normal Distributions across the Sciences: Keys and
640 CluesOn the charms of statistics, and how mechanical models resembling gambling machines offer a link to
641 a handy way to characterize log-normal distributions, which can provide deeper insight into var. *BioScience*,
642 51, 341–352.
- 643 Loehle, C., Li, B.-L. & Sundell, R.C. (1996). Forest spread and phase transitions at forest-prairie ecotones
644 in Kansas, U.S.A. *Landscape Ecology*, 11, 225–235.
- 645 Malhi, Y., Gardner, T.A., Goldsmith, G.R., Silman, M.R. & Zelazowski, P. (2014). Tropical Forests in the
646 Anthropocene. *Annual Review of Environment and Resources*, 39, 125–159.
- 647 Manor, A. & Shnerb, N.M. (2008). Origin of pareto-like spatial distributions in ecosystems. *Physical Review*

- 648 *Letters*, 101, 268104.
- 649 Martensen, A.C., Ribeiro, M.C., Banks-Leite, C., Prado, P.I. & Metzger, J.P. (2012). Associations of Forest
650 Cover, Fragment Area, and Connectivity with Neotropical Understory Bird Species Richness and Abundance.
651 *Conservation Biology*, 26, 1100–1111.
- 652 McKenzie, D. & Kennedy, M.C. (2012). Power laws reveal phase transitions in landscape controls of fire
653 regimes. *Nat Commun*, 3, 726.
- 654 Mitchell, M.G.E., Suarez-Castro, A.F., Martinez-Harms, M., Maron, M., McAlpine, C. & Gaston, K.J. *et al.*
655 (2015). Reframing landscape fragmentation's effects on ecosystem services. *Trends in Ecology & Evolution*,
656 30, 190–198.
- 657 Naito, A.T. & Cairns, D.M. (2015). Patterns of shrub expansion in Alaskan arctic river corridors suggest
658 phase transition. *Ecology and Evolution*, 5, 87–101.
- 659 Newman, M.E.J. (2005). Power laws, Pareto distributions and Zipf's law. *Contemporary Physics*, 46, 323–
660 351.
- 661 Oborny, B., Meszéna, G. & Szabó, G. (2005). Dynamics of Populations on the Verge of Extinction. *Oikos*,
662 109, 291–296.
- 663 Oborny, B., Szabó, G. & Meszéna, G. (2007). Survival of species in patchy landscapes: percolation in space
664 and time. In: *Scaling biodiversity*. Cambridge University Press, pp. 409–440.
- 665 Ochoa-Quintero, J.M., Gardner, T.A., Rosa, I., de Barros Ferraz, S.F. & Sutherland, W.J. (2015). Thresholds
666 of species loss in Amazonian deforestation frontier landscapes. *Conservation Biology*, 29, 440–451.
- 667 Ódor, G. (2004). Universality classes in nonequilibrium lattice systems. *Reviews of Modern Physics*, 76,
668 663–724.
- 669 Pardini, R., Bueno, A. de A., Gardner, T.A., Prado, P.I. & Metzger, J.P. (2010). Beyond the Fragmentation
670 Threshold Hypothesis: Regime Shifts in Biodiversity Across Fragmented Landscapes. *PLoS ONE*, 5, e13666.
- 671 Potapov, P., Hansen, M.C., Stehman, S.V., Loveland, T.R. & Pittman, K. (2008a). Combining MODIS
672 and Landsat imagery to estimate and map boreal forest cover loss. *Remote Sensing of Environment*, 112,
673 3708–3719.
- 674 Potapov, P., Yaroshenko, A., Turubanova, S., Dubinin, M., Laestadius, L. & Thies, C. *et al.* (2008b).
675 Mapping the world's intact forest landscapes by remote sensing. *Ecology and Society*, 13.
- 676 Prishchepov, A.V., Müller, D., Dubinin, M., Baumann, M. & Radeloff, V.C. (2013). Determinants of

- 677 agricultural land abandonment in post-Soviet European Russia. *Land Use Policy*, 30, 873–884.
- 678 Pueyo, S., de Alencastro Graça, P.M.L., Barbosa, R.I., Cots, R., Cardona, E. & Fearnside, P.M. (2010).
679 Testing for criticality in ecosystem dynamics: the case of Amazonian rainforest and savanna fire. *Ecology
Letters*, 13, 793–802.
- 680
- 681 R Core Team. (2015). R: A Language and Environment for Statistical Computing.
- 682 Reyer, C.P.O., Rammig, A., Brouwers, N. & Langerwisch, F. (2015). Forest resilience, tipping points and
683 global change processes. *Journal of Ecology*, 103, 1–4.
- 684 Rockstrom, J., Steffen, W., Noone, K., Persson, A., Chapin, F.S. & Lambin, E.F. *et al.* (2009). A safe
685 operating space for humanity. *Nature*, 461, 472–475.
- 686 Rooij, M.M.J.W. van, Nash, B., Rajaraman, S. & Holden, J.G. (2013). A Fractal Approach to Dynamic
687 Inference and Distribution Analysis. *Frontiers in Physiology*, 4.
- 688 Rudel, T.K., Coomes, O.T., Moran, E., Achard, F., Angelsen, A. & Xu, J. *et al.* (2005). Forest transitions:
689 towards a global understanding of land use change. *Global Environmental Change*, 15, 23–31.
- 690 Saravia, L.A. & Momo, F.R. (2017). Biodiversity collapse and early warning indicators in a spatial phase
691 transition between neutral and niche communities. *PeerJ PrePrints*, 5, e1589v4.
- 692 Scanlon, T.M., Caylor, K.K., Levin, S.A. & Rodriguez-iturbe, I. (2007). Positive feedbacks promote power-
693 law clustering of Kalahari vegetation. *Nature*, 449, 209–212.
- 694 Scheffer, M., Bascompte, J., Brock, W.A., Brovkin, V., Carpenter, S.R. & Dakos, V. *et al.* (2009). Early-
695 warning signals for critical transitions. *Nature*, 461, 53–59.
- 696 Scheffer, M., Walker, B., Carpenter, S., Foley, J. a, Folke, C. & Walker, B. (2001). Catastrophic shifts in
697 ecosystems. *Nature*, 413, 591–596.
- 698 Seidler, T.G. & Plotkin, J.B. (2006). Seed Dispersal and Spatial Pattern in Tropical Trees. *PLoS Biology*,
699 4, e344.
- 700 Sexton, J.O., Noojipady, P., Song, X.-P., Feng, M., Song, D.-X. & Kim, D.-H. *et al.* (2015). Conservation
701 policy and the measurement of forests. *Nature Climate Change*, 6, 192–196.
- 702 Sexton, J.O., Song, X.-P., Feng, M., Noojipady, P., Anand, A. & Huang, C. *et al.* (2013). Global, 30-m
703 resolution continuous fields of tree cover: Landsat-based rescaling of MODIS vegetation continuous fields

- 704 with lidar-based estimates of error. *International Journal of Digital Earth*, 6, 427–448.
- 705 Solé, R.V. (2011). *Phase Transitions*. Primers in complex systems. Princeton University Press.
- 706 Solé, R.V. & Bascompte, J. (2006). *Self-organization in complex ecosystems*. Princeton University Press,
- 707 New Jersey, USA.
- 708 Solé, R.V., Alonso, D. & Mckane, A. (2002). Self-organized instability in complex ecosystems. *Philosophical
709 transactions of the Royal Society of London. Series B, Biological sciences*, 357, 667–681.
- 710 Solé, R.V., Alonso, D. & Saldaña, J. (2004). Habitat fragmentation and biodiversity collapse in neutral
711 communities. *Ecological Complexity*, 1, 65–75.
- 712 Solé, R.V., Bartumeus, F. & Gamarra, J.G.P. (2005). Gap percolation in rainforests. *Oikos*, 110, 177–185.
- 713 Staal, A., Dekker, S.C., Xu, C. & Nes, E.H. van. (2016). Bistability, Spatial Interaction, and the Distribution
714 of Tropical Forests and Savannas. *Ecosystems*, 19, 1080–1091.
- 715 Stauffer, D. & Aharony, A. (1994). *Introduction To Percolation Theory*. Taylor & Francis, London.
- 716 Taubert, F., Fischer, R., Groeneveld, J., Lehmann, S., Müller, M.S. & Rödig, E. et al. (2018). Global
717 patterns of tropical forest fragmentation. *Nature*.
- 718 Vasilakopoulos, P. & Marshall, C.T. (2015). Resilience and tipping points of an exploited fish population
719 over six decades. *Global Change Biology*, 21, 1834–1847.
- 720 Villa Martín, P., Bonachela, J.A. & Muñoz, M.A. (2014). Quenched disorder forbids discontinuous transitions
721 in nonequilibrium low-dimensional systems. *Physical Review E*, 89, 12145.
- 722 Villa Martín, P., Bonachela, J.A., Levin, S.A. & Muñoz, M.A. (2015). Eluding catastrophic shifts. *Proceed-
723 ings of the National Academy of Sciences*, 112, E1828–E1836.
- 724 Viña, A., McConnell, W.J., Yang, H., Xu, Z. & Liu, J. (2016). Effects of conservation policy on China's
725 forest recovery. *Science Advances*, 2, e1500965.
- 726 Vuong, Q.H. (1989). Likelihood Ratio Tests for Model Selection and Non-Nested Hypotheses. *Econometrica*,
727 57, 307–333.
- 728 Weerman, E.J., Van Belzen, J., Rietkerk, M., Temmerman, S., Kéfi, S. & Herman, P.M.J. et al. (2012).
729 Changes in diatom patch-size distribution and degradation in a spatially self-organized intertidal mudflat
730 ecosystem. *Ecology*, 93, 608–618.
- 731 Weissmann, H. & Shnerb, N.M. (2016). Predicting catastrophic shifts. *Journal of Theoretical Biology*, 397,

- 732 128–134.
- 733 Wuyts, B., Champneys, A.R. & House, J.I. (2017). Amazonian forest-savanna bistability and human impact.
- 734 *Nature Communications*, 8, 15519.
- 735 Xu, C., Hantson, S., Holmgren, M., Nes, E.H. van, Staal, A. & Scheffer, M. (2016). Remotely sensed canopy
736 height reveals three pantropical ecosystem states. *Ecology*, 97, 2518–2521.
- 737 Zhang, J.Y., Wang, Y., Zhao, X., Xie, G. & Zhang, T. (2005). Grassland recovery by protection from grazing
738 in a semi-arid sandy region of northern China. *New Zealand Journal of Agricultural Research*, 48, 277–284.
- 739 Zinck, R.D. & Grimm, V. (2009). Unifying wildfire models from ecology and statistical physics. *The
740 American naturalist*, 174, E170–85.